Influence of alkyl chain length on charge transport in symmetrically substituted poly(2,5-dialkoxy-*p*-phenylenevinylene) polymers

Sachetan M. Tuladhar, Marc Sims, James Kirkpatrick, Robert C. Maher, Amanda J. Chatten, Donal D. C. Bradley, and Jenny Nelson
Department of Physics, Imperial College London, Prince Consort Road, London SW7 2AZ, United Kingdom

Pablo G. Etchegoin
The MacDiarmid Institute for Advanced Materials and Nanotechnology, School of Chemical and Physical Sciences, Victoria University of Wellington, P.O. Box 600, Wellington, New Zealand

Christian B. Nielsen, Philippe Massiot, Wayne N. George, and Joachim H. G. Steinke
Department of Chemistry, Imperial College London, Prince Consort Road, London SW7 2AY, United Kingdom

(Received 25 June 2008; revised manuscript received 17 September 2008; published 8 January 2009)

We report on the hole transport characteristics, as measured by time of flight, of a family of symmetrically substituted dialkoxy poly(*p*-phenylenevinylene) polymers with different side-chain length. As side-chain length is decreased, the magnitude of the hole mobility μ_h increases while the field dependence of μ_h becomes more positive and the temperature dependence of μ_h becomes stronger. For the shortest side-chain derivative studied, μ_h exceeds 10^{-4} $cm^2\ V^{-1}\ s^{-1}$ at electric fields greater than 10^5 $V\ cm^{-1}$. The trend in magnitude of μ_h with side-chain length is consistent with the expected increase in electronic wave-function overlap as interchain separation decreases, while the trends in electric-field and temperature dependences of μ_h are consistent with increasing site energy disorder. We show that the electrostatic contribution to the site energy difference for pairs of oligomers follows the observed trend as a function of interchain separation, although the pairwise contribution is too small to explain the data quantitatively. Nonresonant Raman spectroscopy is used to characterize the microstructure of our films. We construct spatial maps of the Raman ratio I_{1280}/I_{1581} and confirm an expected decrease in average film density with side-chain extension. The structural heterogeneity in the maps is analyzed but no clear correlation is observed with transport properties, suggesting that the structural variations relevant for charge transport occur on a length scale finer than the resolution of ~ 1 μm.

DOI: 10.1103/PhysRevB.79.035201 PACS number(s): 73.61.Ph, 72.80.Le, 71.20.Rv, 78.30.Jw

I. INTRODUCTION

The application of conjugated polymers (CPs) to light-emitting devices, thin-film electronics, and solar cells is limited in many cases by the relatively low mobilities of charge carriers within the polymer thin films. Although it is widely agreed[1,2] that charge transport is limited primarily by the rate of charge hopping between polymer chains (*interchain* hopping), no adequate theoretical framework exists through which to relate charge mobilities to the chemical structure of the polymer chains. Ultimately, design rules that relate structure to electrical transport properties are needed in order to develop materials that show superior performance in applications.

Experimental studies have demonstrated that mobilities in CPs can vary by orders of magnitude as a result of variations in the polymer chemical structure or physical morphology. Factors include processing-related variables such as backbone conformation (planarity)[3,4] (which determines the effective length of conjugated segments), alignment and packing of neighboring chains,[5–7] chain packing density,[8] as well as the chemical structure[9,10] and molecular weight[11,12] of the conjugated backbone; the side-chain structure, length, sequence,[13] and symmetry;[3] regioregularity;[14] and chemical purity (e.g. Ref. 15). Measured mobilities are commonly analyzed using semiempirical models such as the Gaussian disorder model (GDM).[16] Such models deliver a quantitative description in terms of a limited set of parameters, which is useful for comparative purposes, but the parameters have physical meaning only for a highly stylized model of the solid (hopping sites on a cubic lattice) and have no direct connection to the physical parameters listed above that control the mobility of real CPs. As a result these models cannot be used for predictive purposes. On the other hand, a valid description of the charge hopping rate between molecules (with weak electronic coupling) is available in the form of nonadiabatic Marcus theory,[17] but this expression cannot easily be applied to obtain a net transport rate for hopping within a disordered assembly of large anisotropic molecules. An accurate estimate of mobility could be obtained, in principle, through combined simulations of molecular conformation (e.g., using molecular dynamics) and charge hopping.[18–20] However, this approach requires accurate knowledge of intermolecular and intramolecular interactions as well as vast computational resources to calculate morphologies and transition rates, and the approach quickly becomes impractical except for small molecules in ordered molecular assemblies. A further complication is the physical origin of the site energy disorder in CPs. Previous studies have identified dipolar interactions as a source of energetic disorder in molecularly doped polymers (comprising conjugated molecules dispersed in an inert polymer matrix).[21,22] However, the absence of large permanent dipole moments in CPs and the comparable size of the transport unit compared

to intermolecular distances means that higher-order multipolar interactions must be invoked to accurately describe the electrostatic interactions.[23] To properly relate these interactions to chemical structure, an atomistic picture of the molecular environment is required.

A useful goal would therefore be to identify (at a phenomenological level) those properties of CPs that influence mobility most strongly and find an alternative parametrization to the GDM that is physically appropriate for CPs. This challenge is assisted by recent studies[13,18,19] that indicate that transport pathways are controlled by the fastest interchain hopping points.

In this paper we address the influence of polymer side-chain length on hole mobility for a series of poly(*p*-phenylenevinylene) (PPV) derivatives. The influence of side chains on CP electronic properties is often attributed to their role in determining chain packing, which in turn affects the degree of coplanarity of the backbone. In the case of regioregular polyalkylthiophenes, for example, processing methods which lead to high charge mobility also lead to the formation of ordered microcrystallites,[6] apparently formed as a result of side-chain interdigitation.[24] In the case of PPV polymers, differences in transport behavior between differently substituted polymers have been related to the effect of side-chain symmetry on backbone planarity.[3,4] In this study, we focus on the less well-studied influence of side-chain *length* on charge transport parameters. In order to minimize variability in morphology and interpret the role of side-chain length most simply, i.e., as an indicator of the separation between polymer backbones, we choose to study symmetrically substituted dialkoxy-PPV polymers. Previous studies[25] have shown that unbranched symmetric side chains impart a high degree of intrachain coplanarity and encourage chain aggregation, in contrast to asymmetric side chains which allow more disorder in chain conformation.[3,25]

We find systematic variations with side-chain length in the magnitude, electric-field and temperature dependences of hole mobility, and in the film morphology for the dialkoxy-PPV derivatives with side-chain lengths of one poly(2,5-dimethoxy-*p*-phenylenevinylene), PDMeOPV (abbreviated C1), six poly(2,5-dihexyloxy-*p*-phenylenevinylene), PDHeOPV (C6), and ten poly(2,5-didecyloxy-*p*-phenylenevinylene), PDDeOPV (C10) carbon atoms. We use spectroscopic studies to show that the corresponding variations in derived GDM parameters cannot be explained exclusively in terms of changes in planarity of the backbone. We use quantum chemical calculations to study the parameters that control interchain charge hopping, i.e., the transfer integral J and site energy difference ΔG, in a model of dialkoxy-PPV as a function of interchain separation, following the evidence that charge transport is rate limited by interchain hopping events. To incorporate the effect of disorder, we calculate the distributions of these parameters for large ensembles of pairs of oligomers in random relative orientations but at a fixed distance of closest approach. The observed trends in the transport parameters with side-chain length are broadly consistent with the results of such calculations as a function of interchain separation.

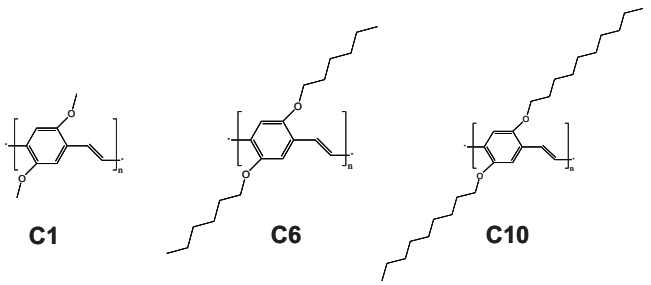

FIG. 1. Chemical structures of PDMeOPV (C1), PDHeOPV (C6), and PDDeOPV (C10).

II. METHODS

A. Experimental

1. Polymer synthesis

The chemical structures of the compounds studied here are shown in Fig. 1. The soluble precursor of PDMeOPV was synthesized by a Wessling-type polymerization of the tetrahydrothiophenium salt (number average molecular weight of 54 kDa, approximately 280 repeat units) and films of PDMeOPV were prepared by thermal conversion of the precursor polymer using the technique described in Ref. 26. Following a previous study of the effect of conversion temperature on optical and electrical properties of the films,[8] the conversion was carried out at 185 °C, under which conditions full elimination of the precursor to the conjugated product is achieved. The soluble polymers, PDHeOPV and PDDeOPV, were prepared by a Gilch-type polymerization of the corresponding 1,4-bis(bromomethyl)-2,5-dialkoxybenzenes. The crude polymers were purified and fractionated by consecutive reprecipitations followed by Soxhlet extractions with pentane and acetone to afford PDHeOPV and PDDeOPV with number average molecular weights of 25 kDa (approximately 82 repeat units) and 35 kDa (approximately 84 repeat units), respectively. Further details on instrumentation, synthetic procedures, and GPC data are provided in the supporting information to the paper.[27]

2. Time-of-flight measurements

In the case of the soluble polymers, C6 and C10, devices were prepared for time-of-flight (ToF) measurements by spin coating solutions of 92 and 100 mg/ml, respectively, of the polymer in chlorobenzene on to indium-tin-oxide (ITO)-coated substrates that had previously been cleaned in ultrasonic bath with acetone and isopropanol. The resulting films were in the range of 1.2–2.3 μm thickness. Devices of area 4.5 mm^2 were defined by thermal evaporation of aluminum top contacts (~100 nm) through a shadow mask. In the case of C1, free-standing films were prepared by the method described in Ref. 8 and aluminum contacts applied to both sides of the films by thermal evaporation. One of the contacts was thin (~30 nm) to enable optical access.

Hole photocurrent transients were measured at a range of applied biases under pulsed (6 ns) illumination through the ITO electrode (C6 and C10) or the semitransparent Al electrode (C1). Measurements were normally performed at 532 nm using the frequency doubled output of a Nd:YAG laser (Quantel). No difference was observed in the hole mobility or its field dependence when the samples were excited at 335 nm. The resulting photocurrent was detected with a digital oscilloscope (Tektronix TDS 3052). The samples were stored *in vacuo* and measured both *in vacuo* and in ambient conditions without any observed effect of atmosphere on the mobility values. Laser pulse intensity was controlled so that the charge generated did not exceed 5%–10% of CV where C is sample capacitance (typically 0.1 nF) and V is the applied bias, so that we could be confident that we were indeed working in a regime where the electric field across the samples can be assumed to be constant.

3. UV-visible, photoluminescence, and Raman spectroscopies

UV-visible (UV-vis) absorption spectra were measured with a Unicam 4 UV/Vis spectrophotometer. Thin films ($d \sim 90$ nm) were prepared for the measurements by spin coating onto Spectrosil B substrates. Photoluminescence (PL) spectra were collected using a SPEX Fluoromax-3 spectrofluorimeter equipped with an accessory for thin-film analysis. Samples were excited at ~450 nm.

Raman measurements were made on a *Renishaw* 2000 charge-coupled-device (CCD)-based instrument equipped with a *BH*-2 Olympus confocal microscope and a *Prior* mapping stage, using a 20 mW 780 nm near-infrared-diode laser excitation source. This excitation wavelength was chosen to avoid exciting background fluorescence. The laser light was focused onto the sample with a ×50 objective to produce a beam of diameter ≈1 μm at the focal point. Raman maps (1 μm resolution and 0.1 s integration time) were obtained over 251×251 μm^2 areas for each sample. The Raman peaks were analyzed (*curvefit* for GRAMS) using mixed Gaussian-Lorentzian fits with subtracted backgrounds. Following Ref. 8, the ratio of the Raman peak intensities at 1280 cm^{-1} (assigned to in-plane vibrations) and 1581 cm^{-1} (assigned to phenylene ring stretching) is interpreted as a measure of local chain packing density. The mean and variance of this ratio for each film type are obtained by statistical analysis of all points (63 000 spectra) on the Raman map.

B. Theoretical methods

Detailed theoretical calculations were carried out on hexamers of dimethoxy-*para*phenylenevinylene. Calculations on shorter oligomers were also carried out and yielded similar results to those described here. The geometry of the isolated oligomer is obtained at the B3LYP/6-31g* level using GAUSSIAN 03.[28] Calculations of hole transfer integral and site energy difference were carried out on pairs of oligomers, where the second oligomer was oriented at random and translated with respect to the first. The rotation matrix is defined by three Euler angles, and in order to sample the orientational space uniformly two angles and the cosine of the third are varied uniformly. The polar and azimuthal angles of the translation vector are chosen to lie on a sphere whose radius is varied until the minimum separation between any two atoms on the two oligomers is equal to a desired value d_{min}. J and ΔG are calculated for each pair. The process is repeated 10^5 times for each value of d_{min} and distributions of the J and ΔG values are thus compiled. For each pair of oligomers, the transfer integral J is calculated using an approximation based on molecular-orbital overlap, as described in Ref. 29. The method described in Ref. 29 is computationally efficient and thereby offers advantages over density-functional-theory methods[30] for the analysis of disordered systems. Zerner's intermediate neglect of differential overlap/spectroscopic (ZINDO/S) orbitals for the individual oligomers were calculated using the ZINDO/S Hamiltonian, as implemented in GAUSSIAN 03.[28] The site energy difference ΔG is calculated as the difference in electrostatic interaction energy estimated using distributed multipole analysis (DMA). This approach is introduced in this paper. The DMA approach is necessary both because the oligomers are large compared to their separation and therefore cannot be substituted by a single multipole expansion and because the quadrupole moment of CPs cannot be represented by point charges localized on the atomic centers. In this approach, ΔG is equated to the difference in interaction energies between the case when the positive charge is localized on one of the two oligomers and when it is localized on the other. Charge density distributions for the radical cation and neutral oligomer are calculated at the B3LYP/6-31g* level using GAUSSIAN 03.[28] The distributed multipoles for each molecule are then obtained using a method due to Stone.[31] The interaction energies are calculated including multipoles up to the quadrupole. Inductive interactions are ignored in the calculation of ΔG. The validity of the approach is supported by calculations for stacks of a discotic liquid crystal in Ref. 32, which show that, for that system, the correction in ΔG due to the polarization of the surrounding ensemble is small. In order to study the effect of side-chain length we recalculate the distributions of J and ΔG for values of separation d_{min} between 2.5 and 19 Å.

For each value of d_{min} the 10^5 calculations took roughly 90 min on a single processor of an OPTERON 24X workstation. For comparison, on the same computer a single self-consistent field (SCF) calculation with the ZINDO/S Hamiltonian on a pair of oligomers of PPV takes roughly 2 min, implying that 10^5 calculations would require roughly one month. The use of the molecular-orbital overlap approximation[29] in place of SCF therefore enables a much larger parameter space to be explored.

III. RESULTS AND DISCUSSION

ToF mobility measurements

Typical ToF hole photocurrent transients for all three polymers at the same applied electric field of 1.7×10^5 V cm^{-1} are shown in Fig. 2(a). In the case of C10, after an initial decay, the photocurrent settles to a constant (plateau) value before falling abruptly toward zero at a

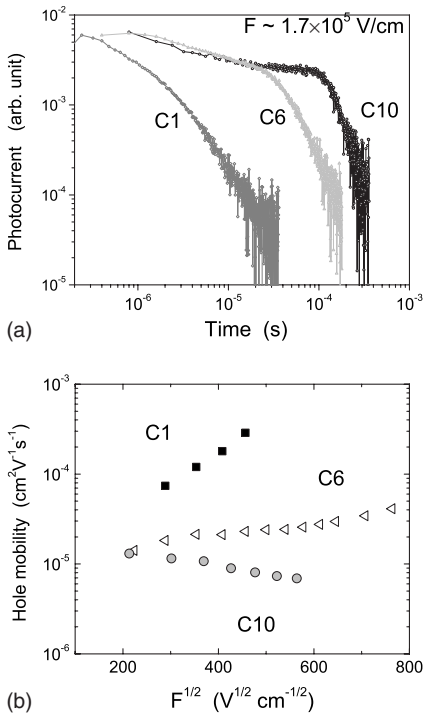

FIG. 2. (a) Room-temperature hole photocurrent transients for all three polymers at an applied field of 1.7×10^5 V cm^{-1} plotted on double-logarithmic axes. (b) Poole-Frenkel plot of room-temperature hole mobility as a function of applied electric field for all three polymers.

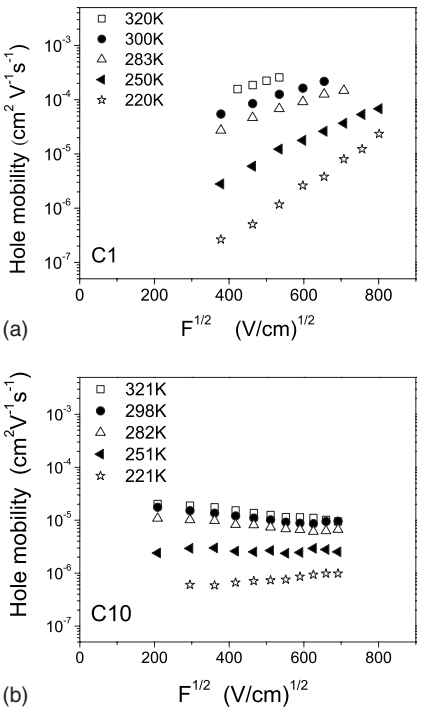

FIG. 3. Poole-Frenkel plots of ToF hole mobilities for (a) C1 and (b) C10 polymers as a function of electric field for temperatures between 220 and 320 K. (Only selected temperatures are shown for clarity.)

distinct knee. Such a transient shape is characteristic of nondispersive charge transport. The nondispersive transient also demonstrates the high quality of the polymer sample since high levels of impurities with energy levels within the transport density of states gap are likely to cause charge trapping. In the case of C6 the plateau region is absent and the knee is less pronounced while in the case of C1 the transient shows a featureless decay, even on a log-log plot, indicating very dispersive transport. The transients become faster as side-chain length decreases, indicating increasing hole mobility. Hole mobility μ_h is determined from the relation

$$\mu = L/t_{\mathrm{tr}}F,$$

where L represents the film thickness, F the electric field, and t_{tr} the transit time. For dispersive transients t_{tr} is defined as the point of intersection of two asymptotes drawn to the transient (plotted in logarithmic representation) at long and short times. Although this definition can overestimate mobility relative to the case where t_{tr} is identified with the point of inflection of a nondispersive transient, it is chosen here because it can be used consistently for both dispersive and nondispersive transients. Room-temperature hole mobilities are plotted as a function of electric field F for the three polymers in Fig. 2(b). Again a clear trend with side-chain length is visible. For fields greater than 4×10^4 V cm^{-1}, hole mobility decreases in the order $\mu_{\mathrm{C1}}>\mu_{\mathrm{C6}}>\mu_{\mathrm{C10}}$ while the field dependence of mobility becomes less positive as mobility decreases. The negative-field dependence of the hole mobility of C10 is characteristic of materials where the degree of energetic disorder is small compared to the degree of positional disorder[16] (as discussed below) and is consistent with the nondispersive transport. In the case of C1, μ_h exceeds 10^{-4} cm^2 V^{-1} s^{-1} for fields greater than 1×10^5 V cm^{-1}. As previously reported,[8] this is the highest hole mobility observed for a PPV polymer.

In a hopping picture, the shape of ToF transients and the dependence on electric field are both influenced by the degree of disorder in site energies and by the variation in the electronic transfer integral between transport units. To quantify the degree of disorder we study the temperature dependence of μ. Figures 3(a) and 3(b) show Poole-Frenkel plots of μ_h over temperatures from 220 to 320 K for C1 and C10, respectively. μ_h is more sensitive to temperature for C1 than C10, varying by 4 orders of magnitude over the studied temperature range for C1 but only by 2 orders for C10, and the more positive electric-field dependence of μ_h for C1 than C10 is maintained over the whole temperature range. Sensitivity of mobility to temperature T is interpreted in many models as an indicator of energetic disorder. To quantify the disorder for these materials we analyze the $\mu_h(F,T)$ data according to the GDM.[16] Although the GDM is based on a model which is a crude approximation to charge transport in CPs, (i.e., Miller-Abrahams hopping on a cubic lattice) it enables a comparison of different materials even though the numbers extracted may not be physically meaningful. Accordingly, the $\mu_h(F,T)$ data for the three polymers are fit to the expression

TABLE I. GDM parameters μ_0, σ, and Σ obtained from analysis of hole mobility data for the three polymers, as well as the mean and standard deviation (SD) of the ratio of Raman peak intensities.

Material	μ_0 (cm^2/Vs)	σ (eV)	C $(cm/V)^{1/2}$	Σ	Mean Raman ratio	SD in Raman ratio
C1	0.25	0.110	5.1×10^{-4}	2.00	0.57	0.097
C6	4.5×10^{-3}	0.091	3.20×10^{-4}	3.05	0.51	0.012
C10	2.7×10^{-4}	0.085	3.26×10^{-4}	3.92	0.47	0.015

$$\mu(T,F) = \mu_0 \exp\left[-\left(\frac{2\sigma}{3kT}\right)^2\right] \times \begin{cases} \exp\left[C\left(\left(\frac{\sigma}{kT}\right)^2 - \Sigma^2\right)\sqrt{F}\right], & \Sigma \geq 1.5 \\ \exp\left[C\left(\left(\frac{\sigma}{kT}\right)^2 - 2.25\right)\sqrt{F}\right], & \Sigma < 1.5 \end{cases} \quad (1)$$

by the procedure described in Ref. 33, where μ_0, σ, Σ, and C are fitting parameters and k is the Boltzmann constant. The results are shown in Table I. These show that as chain length decreases, the zero-field mobility μ_0 increases, the energetic disorder σ increases, and the so-called configurational disorder Σ decreases. In the context of the GDM, μ_0 is a measure of the strength of the intermolecular wave-function overlap (or transfer integral), σ of the disorder in hopping site energies, and Σ of the disorder in transfer integrals arising from variations in molecular orientation. While it is clear that shorter side chains should lead to stronger electronic wave-function overlap it is not immediately clear how side-chain length should influence the distribution of site energies.

Differences in site energy in CPs may result from a complex set of factors, such as variations in backbone structure through their effect on conjugation length, and variations in electrostatic or other intermolecular interactions, while configurational disorder is affected by the order in chain packing, by film density and again by backbone structure. For symmetrically substituted dialkoxy-PPVs, as studied here, a relatively high degree of packing order is expected to be possible, with a high degree of coplanarity and relatively long conjugation lengths.[3] In the case of C1 in particular, large (10–100 μm) crystalline domains have been observed[8,34] while in the case of poly(2,5-dinonyloxy-*p*-phenylenevinylene), PDNoOPV, (C9) liquid crystalline behavior has been reported.[35] Optical absorption and PL spectra for the three polymers [Fig. 4(a)] were compared in order to look for evidence of a trend in conjugation length with side-chain length. All the PL spectra show well-defined vibronic structure, and we find the optical spectra of C6 and C10 to be largely indistinguishable. This similarity indicates that the increase in side-chain length has an insufficiently strong impact on interchain electronic correlations to perturb the essentially intrachain wave function of the emissive excitons. Furthermore, any differences between the polymers in torsional disorder are insufficient to affect the effective conjugation length of the emitting chain segments. In the case of C1, the absorption spectrum is broadened, and peaks at a slightly shorter wavelength than C6 or C10 while the 0-0 emission peak is redshifted by ~20 nm. The larger apparent Stokes shift in C1 relative to C6 and C10 may be indicative of a broadening in the distribution of conjugation lengths, leading to more pronounced spectral diffusion. Such broadening would be consistent with an increase in energetic disorder σ. However, C1 is known to crystallize,[8,34] and crystalline domains are normally associated with narrower distributions of conjugation lengths and hence lower site energy disorder. This apparent contradiction may be resolved by considering the microstructural heterogeneity in C1 films. These films are polycrystalline in nature and the contrast between their disordered glassy interphases and the crystallites is likely to admit large variations in site energy. This heterogeneity is not considered by the GDM and complicates the interpretation of transport behavior in terms of a single location-invariant disorder parameter.[8] In such films it is considered that absorption samples the ensemble of all chain segments while emission emanates preferentially from those chain segments with the longest effective conjugation lengths that represent minima in the energy landscape, toward which excitons migrate and at which they become trapped.

As a probe of the heterogeneity of chain packing, we mapped the Raman spectra for films of all three polymers over an area of 251×251 μm^2. With an estimated sampling depth of 1 μm, Raman acts as a structural probe of the morphology of the whole film. The Raman spectrum of C1 (c.f. Ref. 8) is compared with those of C6 and C10 in Fig. 4(b) with all three spectra showing the same basic features. The two strongest peaks close to ~1280 and ~1580 cm^{-1} are assigned to an intraplane backbone vibration and a phenylene quadrant ring stretching vibration, respectively.[8] While the Raman spectra of the two soluble polymers (C6 and C10) are, like the optical data, effectively indistinguishable, the peak of the quadrant ring stretch mode for C1 is shifted to a lower frequency ($\Delta\sim3$ cm^{-1}) and is more inhomogeneously broadened than those of C6 and C10, while the intraplane vibration mode is also very slightly redshifted. This is taken as evidence for the existence of a proportion of chains with longer effective conjugation lengths in C1 than in the soluble derivatives and is consistent with the PL data. An increased effective conjugation length in C1 could result from hydrogen-bonding-promoted planarization of PDMeOPV chains in the crystalline phase.[34] The inhomogeneous broadening indicates that the greater disorder in C1 continues on a submicron length scale, a conclusion in agreement with reported crystallite dimensions for PDMeOPV.[34] A spatial probe with nanoscale sensitivity would therefore seem to be necessary to fully unravel the morphological dis-

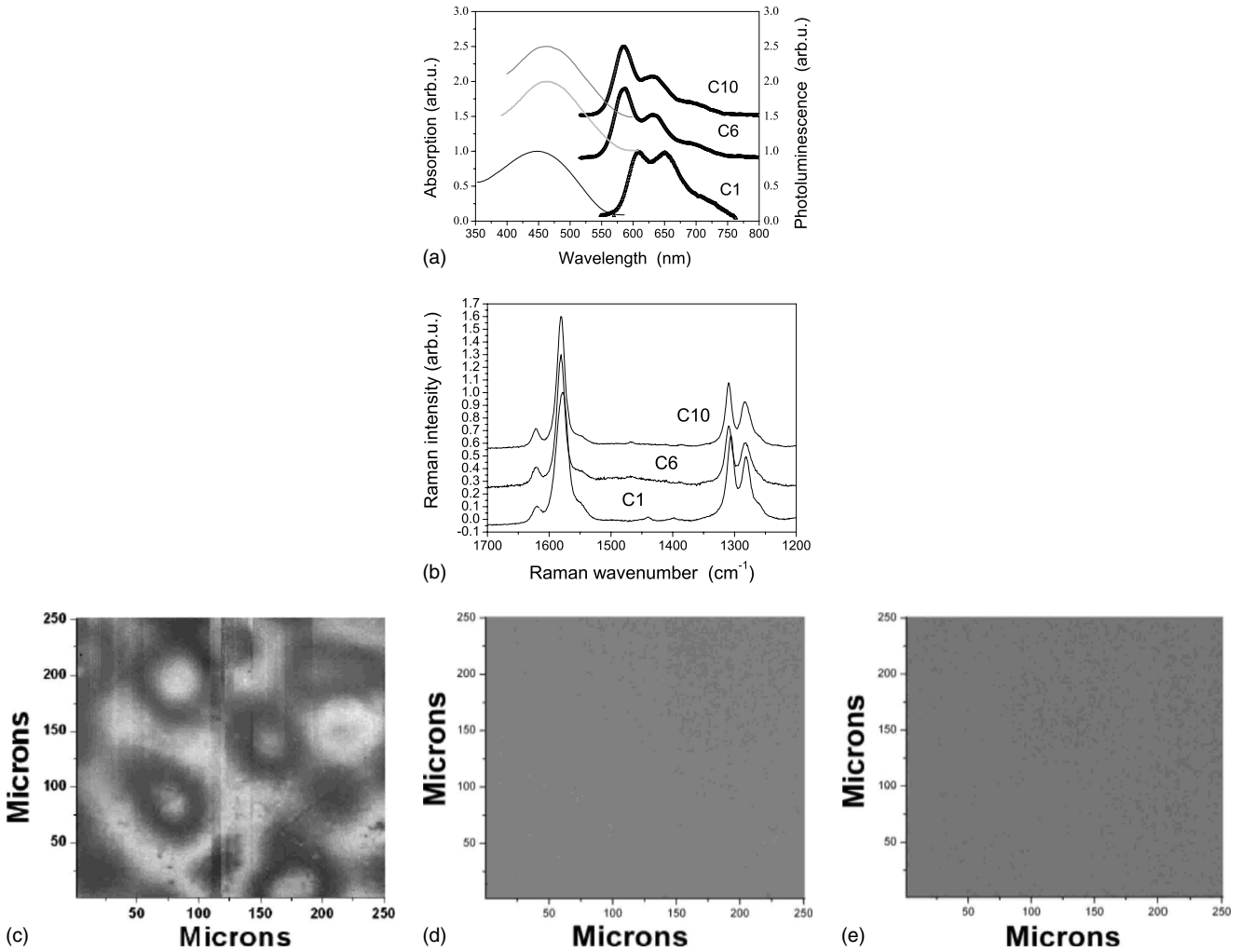

FIG. 4. (a) Absorption and PL spectra for thin films of all three polymers. Spectra are offset vertically for clarity. (b) Raman spectra for the three polymers. [(c)–(e)] Maps of the ratio of the Raman peak intensity at 1280 cm^{-1} to that at 1581 cm^{-1} for 250×250 μm^2 areas on the 1.2–2.3 μm-thick ToF samples of (c) C1, (d) C6, and (e) C10 polymer films. The Raman spectrum for C1 in (b) is taken from a bright region of the Raman map where the Raman ratio is locally high.

tinctions between C1, C6, and C10 films. In addition to supporting the proposed difference in effective conjugation length distribution, the ring stretch mode broadening may also be contributed to by a wider variation in electrostatic environment in C1 compared to C6 and C10. This wider variation would be expected from the inhomogenous domain structure of C1 and, as discussed below, multipolar electrostatic interactions present one cause of energetic disorder in polymers.

Maps of the ratio I_{1280}/I_{1581} of the Raman peak intensity at 1280 cm^{-1} to that at 1581 cm^{-1} for films of C1, C6, and C10 are presented in Figs. 4(c)–4(e). In Ref. 8 it was shown that the relative height of these peaks correlates with the chain packing density. As indicated by the greater contrast in the case of C1 [Fig. 4(c)], where a clear domain structure is evident, this material shows greater heterogeneity in packing density than either C6 or C10 [Figs. 4(d) and 4(e)], which is entirely consistent with its polycrystalline morphology. The absence of contrast in the maps for C6 and C10 is similarly consistent with their more glassy morphology. Indeed, a statistical analysis of the data for all three samples shows that the mean Raman ratio indicates an overall decrease in density with increasing side-chain length and that the standard deviation in the Raman ratio is also significantly lower for the longer side-chain length polymers. Assuming the I_{1280}/I_{1581} Raman ratio to be an indicator of local film density,[8] it might therefore be applied as a probe of configurational disorder. However, given the approximate micron resolution, this disorder likely exists on a length scale far greater than that relevant to charge hopping. This could explain why the parameter Σ obtained by GDM analysis opposes the trend in heterogeneity evidenced by the Raman ratio. The trend in mean packing density deduced from the Raman maps is entirely compatible with the increased density expected upon reducing side-chain length, but the Raman data offer no obvious explanation for the trend in the energetic disorder or configurational disorder parameters, apart from providing evidence for domain boundaries which are likely to be associated with disordered interphases. The Raman-deduced density decrease with increasing side-chain length is however in agreement with the overall reduction in hole mobility.

According to the optical data above, C1 films are more disordered in relation to absorbing and emitting state energies, with a broader distribution of conjugation lengths than the soluble derivatives. There is, however, no evidence to suggest any difference between the distribution of conjugation lengths in films of C6 and C10. In a simplistic picture where the corresponding transport site energy disorder is controlled exclusively by variations in effective conjugation length, these results would imply equal degrees of transport site energy disorder for films of C6 and C10 and therefore no difference in the temperature or electric-field dependence of their mobility. However, experimental results for the soluble derivatives reveal significant differences (see Table I). Alternative sources of energetic disorder, beyond changes in conjugation length, must therefore be considered.

In order to explore the relationship between charge transport parameters and side-chain length, we calculate the parameters controlling the intermolecular hopping rate for pairs of oligomers. We select a "hexamer" of dimethoxy-PPV (with six dimethoxy-phenylene rings and five vinylene linkages) as the transport unit, as this oligomer length is comparable with the expected polaron localization length in PPV.[36] We assume that the rate of hole transport is limited by the rate of the fastest interchain hops (in accordance with Refs. 13 and 19) and that the side-chain length correlates to the shortest separation between two polymer chains (but does not itself define it). Accordingly, we calculate distributions of the hole transfer integral J (from calculation of molecular-orbital overlap) and of the electrostatic site energy difference ΔG (from atomistic calculation of distributed multipole interactions), as functions of the minimum separation $d_{\min}$ between two hexamers, sampling the whole orientational phase space. J and ΔG control the intermolecular transfer rate Γ according to the expression from Marcus-Hush theory[17]

$$\Gamma = \frac{|J|^2}{\hbar}\sqrt{\frac{\pi}{\lambda kT}}\exp\left(-\frac{(\Delta G+\lambda)^2}{4\lambda kT}\right), \tag{2}$$

where λ is the reorganization energy and $\hbar$ is the Planck's constant. The parameters J and ΔG can be related to the GDM parameters in an approximate sense as follows. Equation (1) is obtained from hopping simulations on a cubic lattice where the nearest-neighbor hopping rate is proportional to $e^{-\gamma}$, where γ is distributed on a Gaussian of width Σ, and the rate of upward hops is additionally proportional to $e^{-\Delta G/kT}$, where ΔG is the difference in site energies and the site energies are distributed on a Gaussian of width σ. Thus, we may expect that the GDM parameter μ_0 should relate to $|J|^2$, the variance in ΔG should relate to σ, and the variance in $\log(J)$ should relate to Σ. Below, we examine the trends in the calculated parameters J and ΔG and their variances and compare with trends in the GDM parameters.

Typical distributions of $\log|(J)|^2$ and ΔG obtained from 10^5 random orientations at a minimum separation $d_{\min}$ of 3.5 Å are shown in Fig. 5. The value of $d_{\min}$=3.5 Å was chosen as twice the van der Waals radius of carbon (~1.7 Å), representing the closest approach between face-to-face phenylene rings. Both distributions can be fit to normal distributions, supporting the assumption of the central

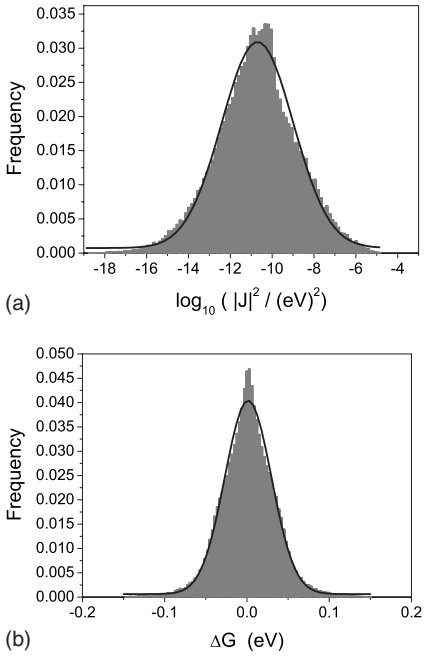

FIG. 5. Frequency plots of (a) the logarithm of the square of the hole transfer integral, $\log_{10}|J|^2$ and (b) the site energy difference ΔG, calculated for a pair of hexamers of dimethoxy-PV at random mutual orientations and a minimum separation of 3.5 Å. Solid lines represent Gaussian fits to the data.

limit theorem intrinsic to the GDM, at least for the case of pairs of molecules. It is important to note that the variation in J is significant, showing that mutual orientation influences the electron transfer rate very strongly; i.e., configurational disorder is important. The value of the standard deviation in ΔG, σ_{DMA}, is smaller than values (0.05–0.15 eV) typically quoted for energetic disorder in organic semiconductors. (Note also that σ_{DMA} should be compared to $\sigma\sqrt{2}$ since σ_{DMA} refers to the variance in the *difference* of site energies rather than the standard deviation in site energy.) However, σ_{DMA} is obtained from the electrostatic interaction of single pairs of nearest neighbors only. Since electrostatic interactions are long ranged, several neighboring molecules would contribute to the local electrostatic potential in a solid film with the result that the net variance in ΔG is much larger than that for a single pair of molecules.

In Figs. 6(a) and 6(b) the root-mean-square value of J, J_{rms}, and the standard deviation of ΔG, σ_{DMA}, respectively, are plotted as functions of separation $d_{\min}$. J_{rms} falls exponentially with a natural length scale of 0.42 Å. The dependence on separation of J_{rms} can be explained by the expected decrease in orbital overlap with increasing intermolecular separation. The distribution of the logarithm of J was also inspected as a function of separation and the standard deviation was found to be almost independent of separation. This makes sense when we note that, although the value of the transfer integral is strongly dependent on relative orientation of the two molecules, the value for any particular orientation decreases with increasing separation with a similar length scale; for the case of fluorene oligomers this is demonstrated in Refs. 19 and 37. In the terminology of the GDM, this behavior implies that the orientational disorder is significant

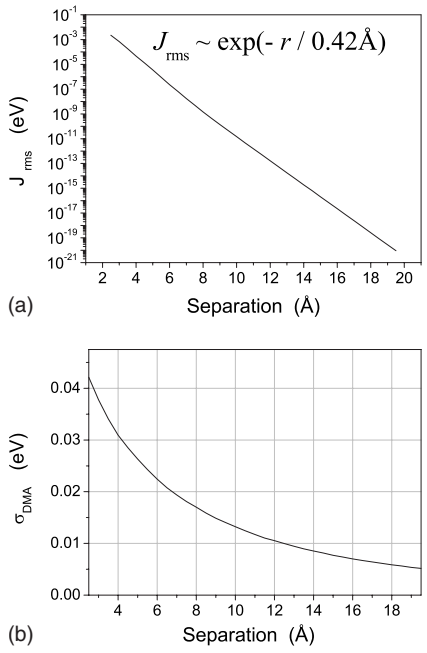

FIG. 6. (a) Root-mean-square hole transfer integral J_{rms} and (b) standard deviation of site energy difference σ_{DMA} as functions of distance of closest approach between two hexamers of dimethoxy-PV.

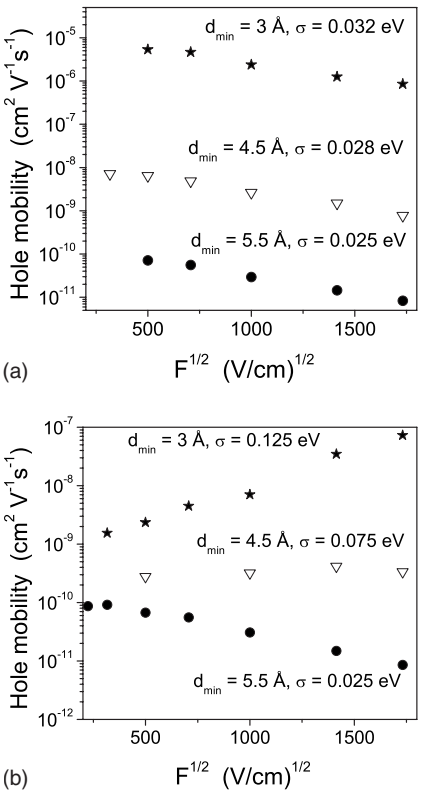

FIG. 7. Simulated ToF hole mobilities for hopping on a cubic lattice with mean and spread of $\log(|J|^2)$ taken from the calculated Gaussian distributions for different interchain separations (a) with site energy disorder taken from Fig. 6(b) and (b) for a wider range of site energy disorder values.

but is independent of intermolecular separation and therefore of side-chain length, in contrast to the trend in configurational disorder implied by the GDM analysis results in Table I. σ_{DMA} also decreases with increasing d_{min} but much more slowly than J_{rms}. The trend in σ_{DMA} can be explained by arguing that the difference in electrostatic interactions is correlated with the absolute values of the two electrostatic interactions and therefore falls with separation. With regard to site energy difference these results indicate that, in the presence of orientational disorder, tighter chain packing leads to greater energetic disorder because of stronger electrostatic interactions. This conclusion can be extended to larger assemblies of molecules. Moreover, we note that this trend would not be affected by including inductive interactions.

Having determined trends in the transport parameters and their distributions with intermolecular separation, we now address the question of whether these results can explain the observed trends in the transport parameters with side-chain length. We take an approach similar to that used in deriving the GDM. ToF photocurrent transients are simulated on a cubic lattice using Monte Carlo simulation,[38] with the intermolecular charge hopping rate given by Eq. (2). Site energies are assigned from a Gaussian distribution of width σ where σ depends on side-chain length, and each site is assigned a contribution Δ to the disorder in $\ln(|J|^2)$ from a Gaussian of width δ [equal to $1/\sqrt{2}$ times the standard deviation of $\ln(|J|^2)$]. The $|J|^2$ value for a transition from site i to site j is then given by $\exp[\langle \ln|J|^2\rangle_d + \Delta(\ln|J|^2)_{\text{site } i} + \Delta(\ln|J|^2)_{\text{site } j}]$, where $\langle \ln|J|^2\rangle_d$ represents the mean of the logarithm of $|J|^2$ for that side-chain length. We use the values of $\langle \ln|J|^2\rangle_d$ and standard deviation in $\ln(|J|^2)$ obtained in the calculations without change (i.e., $\langle \ln|J|^2\rangle_d = -8.7 - 4.5d$, where d is the interchain separation in angstrom, and $\delta = 4/\sqrt{2} = 2.8$). The closest intermolecular separation for a given side-chain length cannot be determined easily, but we argue that the separation between the closest two atoms of a pair of C1 oligomers should be no smaller than 3 Å. In the case of longer side-chain lengths, the closest interchain separation should be longer than for C1 but not as long as the extended length of the alkyl chain. To demonstrate the approximate trends of mobility with side-chain length we choose interchain separations of 3.0, 4.5, and 5.5 Å, respectively, for the C1, C6, and C10 polymers. Note that the aim of this study is not to reproduce the values of mobility absolutely but rather to demonstrate the effects of significant changes in the side-chain length. A cation reorganization energy λ of 0.20 eV is used throughout and calculated according to the approach of Ref. 39 using values of the energy of the neutral and positively charged oligomer in the geometry of the neutral molecule and the cation obtained through hybrid density-functional theory calculations.

The results for simulated room-temperature hole mobility for these interchain separations and energetic disorder values read from Fig. 6(b) of 32, 28, and 24 meV, respectively, are shown in Fig. 7(a). From this plot it is clear that the model reproduces the experimentally observed trend, in which the magnitude of mobility decreases with increasing side-chain length. (No attempt is made to fit the absolute values of mobility.) However, the model does not reproduce the observed variation in field dependence between C1, C6, and

C10; rather the similar small energetic disorder values all lead to a similar weak negative dependence of mobility on field. The different field dependences imply a very large difference in energetic disorder between these cases, and this is not consistent with the weak variation in σ_{DMA} with d_{min} seen in Fig. 6(b). In Fig. 7(b) we present results for a wider range of site energy disorder: $\sigma=25$ meV and $d_{\mathrm{min}}=5.5$ Å for C10, $\sigma=75$ meV and $d_{\mathrm{min}}=4.5$ Å for C6, and $\sigma=125$ meV and $d_{\mathrm{min}}=3.0$ Å for C1. The agreement with the experimental trend in field dependence is improved, indicating that our method underestimates the energetic disorder for short interchain separations. One likely explanation is that our method, which considers only contributions from single neighbors, underestimates the variation in electrostatic interactions. The underestimate would be more severe for short distances when the influence of a larger number of next-nearest neighbors is important. Processes other than the pairwise electrostatic interactions may also influence the true site energy disorder. In addition, the crystalline packing of the molecules in C1 may influence the site energy disorder for example by introducing large variations in pairwise interactions near the domain boundaries. Unfortunately, crystalline systems cannot be modeled considering only pairs of molecules and therefore extension of the study to crystalline or polycrystalline C1 is beyond the scope of this model. Extrinsic defects could also influence the side-chain dependence of energetic disorder since shorter side chains may more easily allow stronger electronic interactions between such defects and the conjugated backbone. Our main result remains that, for systems with an equivalent degree of packing disorder, energetic disorder increases with tighter packing. Thus, the reduction in hole mobility as side-chain length is increased from C1 to C6 to C10 is attributed to a reduction in overlap of the electronic wave function as the conjugated backbones are separated. The reduction in the temperature and positive electric-field dependences of mobility is attributed to a decrease in energetic disorder, which results at least in part from intermolecular electrostatic interactions.

IV. CONCLUSIONS

In conclusion, we have studied the dependence on side-chain length of the time-of-flight hole mobility of symmetrically substituted dialkoxy-PPV polymers. Symmetrically substituted derivatives were chosen in order to maximize the backbone planarity and minimize variations in chain morphology. The magnitude of the hole mobility increases with decreasing side-chain length, following the expected exponential increase in the electronic transfer integral with decreasing interchain separation, and the field dependence of mobility becomes more positive with decreasing side-chain length. For the shortest side-chain derivative studied (C1), the hole mobility exceeds 10^{-4} $\mathrm{cm}^2/\mathrm{V\,s}$ at moderate electric fields.

Analysis of the data with the GDM implies that zero-field mobility and energetic disorder both increase with decreasing side-chain length, while configurational disorder decreases. In order to provide a physical basis for these trends, we evaluated the parameters controlling hopping transport between oligomers of dialkoxy-PPV using electronic structure calculations and calculation of electrostatic interactions through a distributed multipole expansion. As expected, the root-mean-square electronic transfer integral decreases exponentially with the distance of closest approach between oligomers. Less intuitively, the calculated disorder in site energies also decreases with intermolecular separation while the disorder in transfer integral is relatively independent of separation. Monte Carlo simulations showed that the calculated hopping transport parameters predicted the observed trend in the experimental data, although the calculations appear to underestimate the separation dependence of site energy disorder. The latter point can be explained by the neglect in the model of longer range electrostatic interactions with other neighboring molecules in the solid film and the neglect of other possible influences on site energy disorder such as conformational defects. To a first approximation, the variations in transport properties can be explained by the variation in distance of closest backbone approach. This conclusion provides further support for the proposal that charge transport in organic solids is dominated by pathways that make most use of the fastest available intermolecular hopping rates.

Optical data (Uv-vis, photoluminescence, and Raman spectroscopies) were used to investigate the relative degree of order in the films. While C1 was determined to have the most disordered morphology and exhibited the longest effective conjugation length in the series, no discernible difference was found between C6 and C10. This implies that variations in conjugation length distribution were not responsible for the observed differences in energetic disorder between the polymers. Raman maps were built to monitor variations in local density in the polymer films, and the measurements clearly indicated decreasing average density with increasing side-chain length, as expected. However, no clear correlation was found between the heterogeneity of the density, observed on a micron length scale, and the apparent disorder in electronic transfer integral. This suggests that transport is dominated by variations in a smaller length scale; development of probes of structure on intermolecular length scales should enable this point to be addressed in future studies. Variation in the broadening of the peak assigned to the quadrant ring stretch vibration appeared to be compatible with the trend in energetic disorder, suggesting that the Raman spectra could be used to characterize large-scale variations in energetic disorder; this suggestion merits further study.

ACKNOWLEDGMENTS

The authors acknowledge generous financial support from BP Solar (OSCER project) and the Engineering and Physical Sciences Research Council (U.K.) through funding as part of the "Carbon-based Electronics: A National Consortium" (Grant No. GR/R97085) and the Excitonic Supergen Consortium (Grant No. GR/T26559). GPC data have been provided by the EPSRC-GB-funded polymer characterization service managed and run by RAPRA Technology.

[1] Y. Harima, X. Q. Jiang, Y. Kunugi, K. Yamashita, A. Naka, K. K. Lee, and M. Ishikawa, J. Mater. Chem. **13**, 1298 (2003).
[2] D. Hertel and H. Bassler, ChemPhysChem **9**, 666 (2008).
[3] H. C. F. Martens, P. W. M. Blom, and H. F. M. Schoo, Phys. Rev. B **61**, 7489 (2000).
[4] P. Prins, F. C. Grozema, and L. D. A. Siebbeles, Mol. Simul. **32**, 695 (2006).
[5] M. Redecker, D. D. C. Bradley, M. Inbasekaran, and E. P. Woo, Appl. Phys. Lett. **74**, 1400 (1999).
[6] H. Sirringhaus, P. J. Brown, R. H. Friend, M. M. Nielsen, K. Bechgaard, B. M. W. Langeveld-Voss, A. J. H. Spiering, R. A. J. Janssen, E. W. Meijer, P. Herwig, and D. M. de Leeuw, Nature (London) **401**, 685 (1999).
[7] H. Sirringhaus, R. J. Wilson, R. H. Friend, M. Inbasekaran, W. Wu, E. P. Woo, M. Grell, and D. D. C. Bradley, Appl. Phys. Lett. **77**, 406 (2000).
[8] M. Sims, S. M. Tuladhar, J. Nelson, R. C. Maher, M. Campoy-Quiles, S. A. Choulis, M. Mairy, D. D. C. Bradley, P. G. Etchegoin, C. Tregidgo, K. Suhling, D. R. Richards, P. Massiot, C. B. Nielsen, and J. H. G. Steinke, Phys. Rev. B **76**, 195206 (2007).
[9] M. Redecker, D. D. C. Bradley, M. Inbasekaran, W. W. Wu, and E. P. Woo, Adv. Mater. (Weinheim, Ger.) **11**, 241 (1999).
[10] D. Poplavskyy, J. Nelson, and D. D. C. Bradley, Macromol. Symp. **212**, 415 (2004).
[11] C. L. Donley, J. Zaumseil, J. W. Andreasen, M. M. Nielsen, H. Sirringhaus, R. H. Friend, and J. S. Kim, J. Am. Chem. Soc. **127**, 12890 (2005).
[12] R. J. Kline, M. D. McGehee, E. N. Kadnikova, J. S. Liu, J. M. J. Frechet, and M. F. Toney, Macromolecules **38**, 3312 (2005).
[13] B. K. Yap, R. Xia, M. Campoy-Quiles, P. N. Stavrinou, and D. D. C. Bradley, Nature Mater. **7**, 376 (2008).
[14] Y. Kim, S. Cook, S. M. Tuladhar, S. A. Choulis, J. Nelson, J. R. Durrant, D. D. C. Bradley, M. Giles, I. McCulloch, C. S. Ha, and M. Ree, Nature Mater. **5**, 197 (2006).
[15] S. A. Choulis, Y. Kim, J. Nelson, D. D. C. Bradley, M. Giles, M. Shkunov, and I. McCulloch, Appl. Phys. Lett. **85**, 3890 (2004).
[16] H. Bassler, Phys. Status Solidi B **175**, 15 (1993).
[17] K. F. Freed and J. Jortner, J. Chem. Phys. **52**, 6272 (1970).
[18] J. Kirkpatrick, V. Marcon, J. Nelson, K. Kremer, and D. Andrienko, Phys. Rev. Lett. **98**, 227402 (2007).
[19] S. Athanasopoulos, J. Kirkpatrick, D. Martinez, J. M. Frost, C. M. Foden, A. B. Walker, and J. Nelson, Nano Lett. **7**, 1785 (2007).
[20] Y. Olivier, V. Lemaur, J. L. Bredas, and J. Cornil, J. Phys. Chem. A **110**, 6356 (2006).
[21] D. H. Dunlap, P. E. Parris, and V. M. Kenkre, Phys. Rev. Lett. **77**, 542 (1996).
[22] Y. N. Gartstein and E. M. Conwell, Chem. Phys. Lett. **245**, 351 (1995).
[23] S. V. Novikov, J. Polym. Sci., Part B: Polym. Phys. **41**, 2584 (2003).
[24] M. J. Winokur and W. Chunwachirasiri, J. Polym. Sci., Part B: Polym. Phys. **41**, 2630 (2003).
[25] M. Kemerink, J. K. J. van Duren, A. van Breemen, J. Wildeman, M. M. Wienk, P. W. M. Blom, H. F. M. Schoo, and R. A. J. Janssen, Macromolecules **38**, 7784 (2005).
[26] P. L. Burn, D. D. C. Bradley, R. H. Friend, D. A. Halliday, A. B. Holmes, R. W. Jackson, and A. Kraft, J. Chem. Soc., Perkin Trans. 1 1992, 3225.
[27] See EPAPS Document No. E-PRBMDO-78-022847 for further details on instrumentation, synthetic procedures, and GPC data. For more information on EPAPS, see http://www.aip.org/pubservs/epaps.html.
[28] M. J. Frisch, G. W. Trucks, H. B. Schlegel, G. E. Scuseria, M. A. Robb, J. R. Cheeseman, J. A. J. Montgomery, T. Vreven, K. N. Kudin, J. C. Burant, J. M. Millam, S. S. Iyengar, J. Tomasi, V. Barone, B. Mennucci, and M. Cossi, *Gaussian 03 Revision C.02.* (Gaussian, Inc., Wallingford, CT, 2004).
[29] J. Kirkpatrick, Int. J. Quantum Chem. **108**, 51 (2008).
[30] E. F. Valeev, V. Coropceanu, D. A. da Silva, S. Salman, and J. L. Bredas, J. Am. Chem. Soc. **128**, 9882 (2006).
[31] A. J. Stone, J. Chem. Theory Comput. **1**, 1128 (2005).
[32] J. Kirkpatrick, V. Marcon, K. Kremer, J. Nelson, and D. Andrienko, J. Chem. Phys. **129**, 094506 (2008).
[33] T. Kreouzis, D. Poplavskyy, S. M. Tuladhar, M. Campoy-Quiles, J. Nelson, A. J. Campbell, and D. D. C. Bradley, Phys. Rev. B **73**, 235201 (2006).
[34] J. H. F. Martens, E. A. Marseglia, D. D. C. Bradley, R. H. Friend, P. L. Burn, and A. B. Holmes, Synth. Met. **55**, 449 (1993).
[35] M. Hamaguchi and K. Yoshino, Jpn. J. Appl. Phys., Part 2 **33**, L1689 (1994).
[36] Y. Shimoi, S. Abe, S. I. Kuroda, and K. Murata, Solid State Commun. **95**, 137 (1995).
[37] J. L. Bredas, J. P. Calbert, D. A. da Silva, and J. Cornil, Proc. Natl. Acad. Sci. U.S.A. **99**, 5804 (2002).
[38] A. J. Chatten, S. M. Tuladhar, S. A. Choulis, D. D. C. Bradley, and J. Nelson, J. Mater. Sci. **40**, 1393 (2005).
[39] K. Sakanoue, M. Motoda, M. Sugimoto, and S. Sakaki, J. Phys. Chem. A **103**, 5551 (1999).